MCB
Journals.ASM.org

S6 Kinase- and β-TrCP2-Dependent Degradation of p19^{Arf} Is Required for Cell Proliferation

Tadashi Nakagawa,[a] Takaaki Araki,[a,b] Makiko Nakagawa,[a] Atsushi Hirao,[c] Michiaki Unno,[b] Keiko Nakayama[a]

Division of Cell Proliferation, ART,[a] and Department of Surgery,[b] Graduate School of Medicine, Tohoku University, Sendai, Japan; Division of Molecular Genetics, Cancer and Stem Cell Program, Cancer Research Institute, Kanazawa University, Kanazawa, Japan[c]

The kinase mTOR (mammalian target of rapamycin) promotes translation as well as cell survival and proliferation under nutrient-rich conditions. Whereas mTOR activates translation through ribosomal protein S6 kinase (S6K) and eukaryotic translation initiation factor 4E-binding protein (4E-BP), how it facilitates cell proliferation has remained unclear. We have now identified p19^{Arf}, an inhibitor of cell cycle progression, as a novel substrate of S6K that is targeted to promote cell proliferation. Serum stimulation induced activation of the mTOR-S6K axis and consequent phosphorylation of p19^{Arf} at Ser^{75}. Phosphorylated p19^{Arf} was then recognized by the F-box protein β-TrCP2 and degraded by the proteasome. Ablation of β-TrCP2 thus led to the arrest of cell proliferation as a result of the stabilization and accumulation of p19^{Arf}. The β-TrCP2 paralog β-TrCP1 had no effect on p19^{Arf} stability, suggesting that phosphorylated p19^{Arf} is a specific substrate of β-TrCP2. Mice deficient in β-TrCP2 manifested accumulation of p19^{Arf} in the yolk sac and died *in utero*. Our results suggest that the mTOR pathway promotes cell proliferation via β-TrCP2-dependent p19^{Arf} degradation under nutrient-rich conditions.

Cells respond to environmental changes by regulating cellular states such as proliferation, growth, survival, and apoptosis. A sufficient supply of nutrients is required to ensure the protein production necessary for cell proliferation and growth. The serine-threonine kinase mTOR (mechanistic or mammalian target of rapamycin) serves as a sensor of cellular resources and a link between nutrient availability and protein synthesis. This kinase is present in two distinct complexes, mTORC1 and mTORC2, whose activators and targets differ. Whereas mTORC1 is composed of Raptor, PRAS40, and the mTORC core components (mTOR, Deptor, mLST8, Tti1, and Tel2), mTORC2 consists of Rictor, mSin1, and Protor as well as the mTORC core components (1).

The mTORC1 complex is activated by growth factors and nutrients such as amino acids. Growth factors activate mTORC1 via the phosphoinositide 3-kinase (PI3K)–AKT–tuberous sclerosis protein (TSC) pathway, which triggers activation of the mTOR activator Rheb, whereas amino acids activate the Rag family of small GTPases, which mediate the translocation of mTORC1 to the lysosomal surface, where it encounters Rheb (2). Among various proteins phosphorylated by mTORC1, p70 ribosomal protein S6 kinase (S6K) and eukaryotic translation initiation factor 4E (eIF4E)-binding protein (4E-BP) are the best characterized to date. S6K activated by mTORC1 phosphorylates several substrates that function in various steps of translation, including eIF4B, programmed cell death protein 4 (PDCD4), eukaryotic translation elongation factor 2K (eEF2K), and ribosomal protein S6 (3), whereas phosphorylation of 4E-BP by mTORC1 induces the liberation of bound eIF4E and thereby promotes translation initiation (4). Although these various observations clarify how mTORC1 activates translation through S6K and 4E-BP, the molecular mechanism of mTORC2 activation and its key substrates have remained unclear (1).

Compared with translational regulation, the mechanism by which mTOR regulates cell proliferation and the cell cycle is less well understood (1, 5, 6). Such regulation by mTOR has been proposed to be mediated at the level of translation (7) or transcription (8), but direct regulation of proliferation by mTOR has not been revealed to date.

Cell cycle progression requires that the abundance of regulatory proteins be strictly controlled, with protein degradation being thought to play a fundamental role in such orchestrated regulation (9). In eukaryotic cells, protein degradation is mediated by the proteasome and lysosomal proteases. Proteins destined for degradation by the proteasome are specifically marked by covalent attachment of ubiquitin, with an E3 ubiquitin ligase being responsible for substrate selection (10). Some ubiquitin ligases are multiprotein complexes that contain separate modules for binding the substrate and activated ubiquitin. F-box proteins such as β-TrCP constitute the substrate-binding subunits of SCF-type ubiquitin ligase complexes (11).

Whereas β-TrCP is encoded by a single gene in invertebrates, mammalian genomes contain two different genes for β-TrCP1 and β-TrCP2, which share 88% amino acid sequence identity. Given that specific substrates of either β-TrCP1 or β-TrCP2 have not been identified to date, these two paralogs have been thought to be biochemically redundant. Otherwise, >50 proteins have been identified as substrates of β-TrCP1 or β-TrCP2 in mammalian cells, with these proteins including several signaling mole-

Received 2 April 2015 **Returned for modification** 1 June 2015
Accepted 28 July 2015
Accepted manuscript posted online 3 August 2015
Citation Nakagawa T, Araki T, Nakagawa M, Hirao A, Unno M, Nakayama K. 2015. S6 kinase- and β-TrCP2-dependent degradation of p19^{Arf} is required for cell proliferation. Mol Cell Biol 35:3517–3527. doi:10.1128/MCB.00343-15.

Address correspondence to Keiko Nakayama, nakayak2@med.tohoku.ac.jp.
T.N. and T.A. contributed equally to this work.

Supplemental material for this article may be found at http://dx.doi.org/10.1128/MCB.00343-15.

doi:10.1128/MCB.00343-15

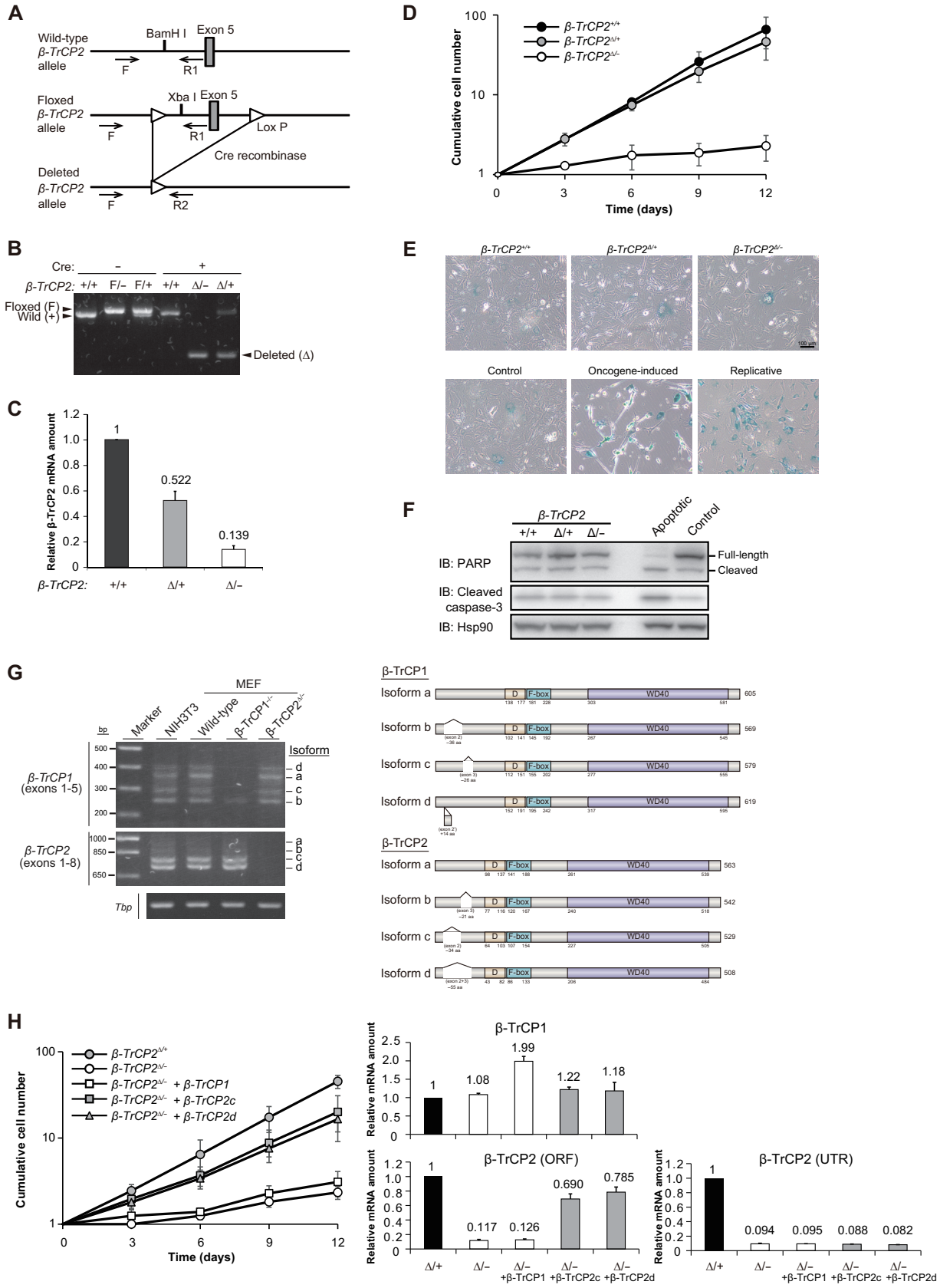

FIG 1 Acute disruption of the β-TrCP2 gene impairs proliferation in MEFs. (A) Structures of the mouse β-TrCP2 gene locus, the floxed (F) allele resulting from homologous recombination in ES cells, and the deleted (Δ) allele resulting from Cre-mediated removal of exon 5 in MEFs. Exon 5 is flanked by loxP sequences

cules, cell cycle regulators, and cell death-related proteins that play key roles in development (12–14). We and others previously showed that disruption of the β-TrCP1 gene did not affect mouse development (15, 16). Accumulation of β-TrCP substrates such as IκB and β-catenin was minimal in primary mouse embryonic fibroblasts (MEFs) derived from the mutant mice, suggesting that β-TrCP2 compensated for the loss of β-TrCP1. To investigate further the function of β-TrCP, we have now analyzed MEFs in which the β-TrCP2 gene was conditionally deleted by Cre recombinase. Our results revealed that β-TrCP2, but not β-TrCP1, mediates the ubiquitylation and degradation of the cell cycle regulator p19^{Arf} after its phosphorylation resulting from activation of the mTOR-S6K axis in response to serum stimulation. We have thus uncovered a novel molecular mechanism by which nutrient availability regulates cell proliferation through degradation of p19^{Arf} and also have revealed a functional difference between β-TrCP paralogs.

MATERIALS AND METHODS

Generation of mutant mice and preparation of MEFs. Cloned DNA corresponding to the β-TrCP2 gene locus was isolated from a 129/Sv mouse genomic library (Stratagene) (17). Targeting vectors were constructed by application of PCR with appropriate primers. The maintenance, transfection, and selection of embryonic stem (ES) cells were performed as described previously (18). Targeted homologous recombination was confirmed by Southern blotting. The mutant ES cells were microinjected into C57BL/6 blastocysts, and the resulting male chimeras were mated with female C57BL/6 mice. The germ line transmission of the mutant allele was also confirmed by Southern blotting. Heterozygous offspring were intercrossed to produce homozygous mutant animals. MEFs were prepared as described previously (16). Cdkn2a knockout mice were kindly provided by A. Hirao (Kanazawa University) with agreement of the Mouse Models of Human Cancers Consortium (MMHCC) (National Cancer Institute—Frederick) (19, 20). All mice were backcrossed to C57BL/6 mice for at least six generations and were maintained in a specific-pathogen-free facility at the Institute of Animal Experimentation, Tohoku University Graduate School of Medicine. They were provided with water and rodent chow *ad libitum* and were treated according to the standards for care and use of laboratory animals of Tohoku University and the guidelines for proper conduct of animal experiments of the Ministry of Education, Culture, Sports, Science, and Technology of Japan. Primers used for genotyping are described in the supplemental material.

RNA isolation, RT-PCR, and RT-qPCR. Isolation of RNA and reverse transcription-quantitative PCR (RT-qPCR) were performed as described previously (21). RNA isolated and purified with the use of an SV total RNA isolation system (Promega) was thus subjected to RT with the use of a PrimeScript RT reagent kit (TaKaRa Bio, Shiga, Japan) followed either by qPCR analysis with a StepOnePlus real-time PCR system (Life Technologies) and Fast SYBR green master mix (Life Technologies) or by agarose gel electrophoresis. For qPCR, data were analyzed according to the $2^{-\Delta\Delta CT}$ method and were normalized by the amount of acidic ribosomal phosphoprotein P0 (Arbp) mRNA. The sequences of PCR primers are provided in the supplemental material.

SA-β-gal staining. Cells (1×10^5 per well) were seeded in six-well plates, cultured for 2 days, washed with phosphate-buffered saline (PBS), and fixed with 0.5% glutaraldehyde in PBS for 10 min at room temperature. They were then washed consecutively with PBS and with PBS (pH 6.0) containing 1 mM $MgCl_2$ before staining for senescence-associated β-galactosidase (SA-β-gal) activity for 16 h at room temperature with PBS (pH 6.0) containing X-Gal (5-bromo-4-chloro-3-indolyl-β-D-galactopyranoside) substrate (650 μg/ml), 1 mM $MgCl_2$, 5 mM K_3FeCN_6, and 5 mM K_4FeCN_6.

Cell culture and viral infection. 293T cells, MEFs, and NIH 3T3 cells were maintained in Dulbecco's modified Eagle's medium supplemented with 10% fetal bovine serum, penicillin (50 U/ml), streptomycin (50 μg/ml), 2 mM L-glutamine, 1% MEM nonessential amino acids, and 1% sodium pyruvate (all from Life Technologies). Conditional deletion of the β-TrCP2 gene in MEFs was achieved by infection with a retrovirus containing Cre recombinase and puromycin resistance genes. The pMX-puro-Cre vector was introduced into Plat-E packaging cells (22) by transfection with the FuGENE6 reagent (Promega), and culture supernatants containing retroviruses were recovered, diluted, and applied to proliferating MEFs in the presence of Polybrene (1 μg/ml). The infected cells were then subjected to selection in medium containing puromycin (2.5 μg/ml) for 3 days. Retroviruses encoding mouse Ras^{G12V}, p19^{Arf}, β-TrCP1 isoform a, or β-TrCP2 isoform c or d were also similarly produced for cell infection. Retrovirus-mediated stable knockdown of p19^{Arf} was performed with the use of blasticidin (10 μg/ml) for selection. The target sequences for the short hairpin RNAs (shRNAs) shp19-1, -2, and -3 were 5′-GCGUGUCUAGCAUGUGGCUUU-3′, 5′-GCUCUGGCUUUCGUGAACAUG-3′, and 5′-GCAGGUUCUUGGUCACUGUGA-3′, respectively.

Plasmid construction and transfection. cDNAs encoding p19^{Arf}, β-TrCP1 isoform a, and β-TrCP2 isoforms c and d were amplified from a cDNA library derived from MEFs and cloned into the pENTR vector (Invitrogen). cDNA encoding human p14^{Arf} was amplified from a cDNA library derived from 293T cells. The LR reaction was performed as described previously (23). Point mutations were introduced by PCR-based site-directed mutagenesis. Transient transfection of 293T cells with plasmid DNA was performed as described previously (24).

Immunoprecipitation and immunoblot analysis. For immunoprecipitation, cells were washed with PBS and lysed by incubation for 10 min at 4°C in a solution containing 0.5% Nonidet P-40 (NP-40), 50 mM Tris-HCl (pH 7.5), 150 mM NaCl, 10% glycerol, a protease inhibitor cocktail (aprotinin [10 μg/ml; Sigma], leupeptin [10 μg/ml; Peptide Institute],

(triangles) in the floxed allele. Genotyping primers (F, R1, and R2) are indicated by arrows. (B) Genomic PCR analysis of MEFs of the indicated β-TrCP2 genotypes at 4 days after infection with a retrovirus encoding Cre recombinase or the corresponding empty virus. (C) RT-qPCR analysis of β-TrCP2 mRNA in MEFs of the indicated genotypes at 4 days after infection with a retrovirus for Cre recombinase. The PCR primers were targeted to the region spanning exons 4 and 5. Data are means ± standard errors of the means (SEM) for two independent experiments. (D) Time course of MEF proliferation beginning 4 days after Cre retrovirus infection. Data are means ± SEM for three independent experiments. (E) SA-β-gal staining of MEFs of the indicated β-TrCP2 genotypes. Oncogene-induced senescent MEFs were prepared by infection with a retrovirus encoding Ras^{G12V}. Replicative senescent MEFs were obtained after culture for eight passages. Control MEFs were prepared by infection with a retrovirus with empty vector. Scale bar, 100 μm. (F) Immunoblot (IB) analysis of poly(ADP-ribose) polymerase (PARP) and the cleaved form of caspase-3 in cell lysates prepared from MEFs of the indicated β-TrCP2 genotypes. Apoptotic MEFs were prepared by treatment with bleomycin (40 μg/ml) for 24 h. Hsp90 was examined as a loading control. (G) Left, RT-PCR analysis of β-TrCP1 and β-TrCP2 mRNAs in NIH 3T3 cells and MEFs of the indicated genotypes. Exons 1 to 5 of β-TrCP1 mRNA and exons 1 to 8 of β-TrCP2 mRNA were amplified, and the PCR products were confirmed by sequencing. Tbp mRNA served as a control. Right, schematic representation of the mouse β-TrCP1 and β-TrCP2 isoforms expressed in MEFs. D, dimerization domain; F-box, F-box domain; WD40, WD40 domain. (H) Left, time course of the proliferation of MEFs of the indicated β-TrCP2 genotypes infected with retroviruses encoding β-TrCP1 isoform a or β-TrCP2 isoform c or d (or with the corresponding empty virus). The cells were infected first with the retroviruses for β-TrCP and then with those for Cre recombinase. Data are means ± SEM for three independent experiments. Right, RT-qPCR analysis of β-TrCP1 and β-TrCP2 mRNAs in the MEFs. Total β-TrCP2 mRNA was measured with primers targeted to the open reading frame (ORF), whereas endogenous β-TrCP2 mRNA was measured with primers targeted to the 3′ untranslated region (UTR). Data are means ± SEM for two independent experiments.

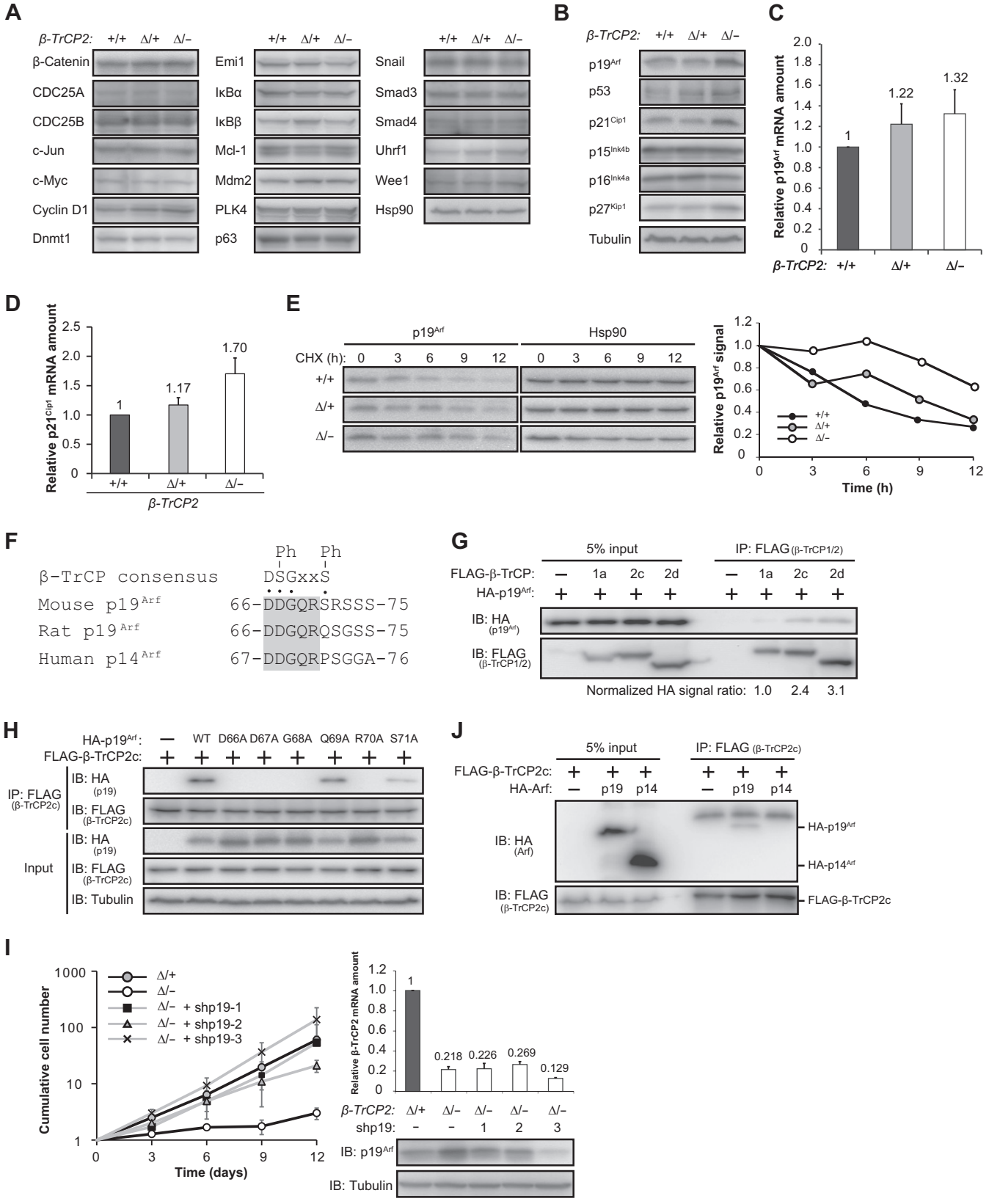

FIG 2 Accumulation of $p19^{Arf}$ is responsible for the arrest of proliferation in β-TrCP2-deficient MEFs. (A) Immunoblot analysis of β-TrCP substrates in MEFs of the indicated genotypes. Hsp90 served as a loading control. (B) Immunoblot analysis of cell cycle inhibitors in MEFs of the indicated genotypes. Tubulin served as a loading control. Data are representative of two independent experiments. (C) RT-qPCR analysis of $p19^{Arf}$ mRNA in MEFs of the indicated β-TrCP2 genotypes. Data are means ± SEM for two independent experiments. (D) RT-qPCR analysis of $p21^{Cip1}$ mRNA in MEFs of the indicated β-TrCP2 genotypes. Data

and phenylmethylsulfonyl fluoride (1 mM; Wako), and a phosphatase inhibitor cocktail (0.4 mM sodium orthovanadate [Wako], 0.4 mM EDTA [Dojindo], 10 mM NaF [Wako], and 10 mM sodium pyrophosphate [Sigma]). The lysates were centrifuged at 20,400 × *g* for 15 min at 4°C, and the resulting supernatants were incubated for 60 min at 4°C with antibody-conjugated Dynabeads protein G (Life Technologies). The immune complexes were then washed three times with PBS containing 0.1% Triton X-100 and 10% glycerol before SDS-polyacrylamide gel electrophoresis and immunoblot analysis. For direct immunoblot analysis, total cell lysates were prepared with radioimmunoprecipitation assay (RIPA) buffer (50 mM Tris-HCl [pH 8.0], 0.1% SDS, 150 mM NaCl, 1% NP-40, 0.5% sodium deoxycholate, and protease inhibitor cocktail). Immunoblot signal intensity was quantified with the use of ImageJ software (version 1.19i). Antibodies for immunoprecipitation and immunoblot analysis are listed in the supplemental material.

Kinase and proteasome inhibitors. LY294002 and rapamycin were obtained from Cell Signaling. U0126, SB203580, glycogen synthase kinase (GSK) inhibitor, and MG132 were from Promega, Wako, Millipore, and Peptide Institute, respectively.

Ubiquitylation assays. For assay of *in vivo* ubiquitylation, cell lysates were prepared with RIPA buffer and subjected to immunoprecipitation with antibodies to p19^{Arf} followed by immunoblot analysis with antibodies to ubiquitin. *In vitro* ubiquitylation assays were performed as described previously (23–25). *Escherichia coli* (BL21) cells transformed with a pET30a plasmid encoding wild-type (WT) or S75A mutant forms of mouse p19^{Arf} were cultured at 37°C to an optical density at 600 nm of 1.0. The temperature was then lowered to 30°C, and the cells were exposed to 0.1 mM isopropyl-β-D-1-thiogalactopyranoside for 6 h, harvested, and then lysed with the use of B-PER (Thermo Scientific). After removal of debris by centrifugation, the lysates were incubated with Ni^{2+}-nitrilotriacetic acid (NTA) beads (Amersham Biosciences) to precipitate His_6-tagged p19^{Arf}, which was then eluted with 250 mM imidazole. The E2 enzymes UBE2D1 and UBE2R1 were produced and purified as for p19^{Arf}. For preparation of SCF$^{β\text{-}TrCP2}$, FLAG-tagged mouse β-TrCP2 (isoform c) and associated proteins were immunoprecipitated from transfected 293T cells with antibodies to FLAG, washed three times with the NP-40 lysis buffer described above and twice with a solution containing 25 mM Tris-HCl (pH 7.5), 50 mM NaCl, 1 mM EDTA, 0.01% NP-40, and 10% glycerol, and then eluted by incubation with a molar excess of the FLAG peptide. An NH_2- and COOH-terminally deleted (constitutively active) form of mouse S6K1 (26) was purified as for SCF$^{β\text{-}TrCP2}$. Various combinations of S6K1, E1 (100 ng; Boston Biochem), E2 (50 ng of UBE2D1 and 100 ng of UBE2R1), and E3 (SCF$^{β\text{-}TrCP2}$) were mixed with 100 ng of recombinant p19^{Arf} in 20 μl of a reaction buffer containing 10 μg of bovine ubiquitin (Sigma), 2 mM ATP, 1 mM $MgCl_2$, 0.3 mM dithiothreitol, 25 mM Tris-HCl (pH 7.5), 120 mM NaCl, 0.5 U of creatine phosphokinase (Sigma), and 1 mM phosphocreatine (Sigma). Reactions were performed for 120 min at 37°C and terminated by boiling for 5 min in SDS sample buffer containing 5% 2-mercaptoethanol, and the mixtures were then subjected to immunoblot analysis with antibodies to p19^{Arf}.

***In vitro* phosphorylation assays.** *In vitro* phosphorylation of p19^{Arf} by S6K1 was performed as described previously (27). In brief, recombinant WT or S75A forms of mouse p19^{Arf} were incubated for 5 min at 37°C with constitutively active S6K1 in 20 μl of kinase assay buffer (25 mM Tris-HCl [pH 7.6], 20 mM $MgCl_2$, 10 mM β-glycerophosphate, 1 mM dithiothreitol, 0.1 mM ATP). The reaction mixtures were then subjected to immunoblot analysis with antibodies to the phosphorylated RXRXXS sequence.

RESULTS

Acute disruption of the β-TrCP2 gene induces proliferation arrest in MEFs. To investigate the physiological function of β-TrCP2, we first disrupted the β-TrCP2 gene in mice. We found that the β-*TrCP2*$^{-/-}$ mice died before embryonic day 10.5 (E10.5) (see Fig. 4E). To circumvent this lethality of gene knockout, we generated mice with a floxed β-*TrCP2* allele. A linearized targeting vector with exon 5 of the β-TrCP2 gene flanked by loxP sequences (floxed) was introduced into ES cells, which were then injected into mouse blastocysts (Fig. 1A). The resulting chimeric males were mated with females to yield heterozygotes. Exon 5 of the mouse β-TrCP2 gene encodes the F-box domain (Fig. 1G), which is necessary for binding to the SKP1 and CUL1 scaffolding proteins of the SCF complex. Deletion of exon 5 thus results in loss of the F-box domain as well as in a codon frameshift in the WD40 domain, which is necessary for association of β-TrCP2 with substrates. Such deletion therefore gives rise to a functional null allele.

To examine the primary effects of β-TrCP2 loss and the cellular mechanism of the associated embryonic lethality, we first prepared MEFs with β-*TrCP2*$^{+/+}$, β-*TrCP2*$^{F/+}$, or β-*TrCP2*$^{F/-}$ genotypes from E13.5 embryos derived from crosses of β-*TrCP2*$^{F/+}$ and β-*TrCP2*$^{+/-}$ mice and then infected the cells with a retrovirus encoding Cre recombinase to delete the floxed allele (yielding the Δ allele). Efficient deletion of exon 5 of the gene was confirmed by PCR analysis of genomic DNA (Fig. 1B), and it was found to result in a marked reduction in the amount of β-TrCP2 mRNA by RT-qPCR analysis (Fig. 1C). Cell proliferation was markedly attenuated in the β-*TrCP2*$^{Δ/-}$ MEFs (Fig. 1D) without any evidence of cellular senescence (Fig. 1E) or apoptosis (Fig. 1F), and this defect was corrected by infection with a retrovirus encoding a β-TrCP2 isoform (c or d) expressed in MEFs (Fig. 1G) but not by overexpression of β-TrCP1 (Fig. 1H). These data thus indicated that β-TrCP2 is required for cell proliferation and has a function distinct from that of β-TrCP1 in MEFs.

Acute disruption of the β-TrCP2 gene induces accumulation of p19^{Arf} in MEFs. Given that most protein ubiquitylation results in protein degradation by the proteasome, loss of β-TrCP2 would be expected to prevent ubiquitylation mediated by this F-box protein and thereby to induce accumulation of its substrates. To characterize the molecular basis of the proliferation arrest induced by β-TrCP2 ablation, we therefore examined the abundances of var-

are means ± SEM for two independent experiments. (E) Left, immunoblot analysis of p19^{Arf} in MEFs of the indicated genotypes incubated with cycloheximide (CHX) (25 μg/ml) for the indicated times. Right, relative p19^{Arf} abundance normalized by Hsp90 abundance as determined by quantitation of immunoblot signals. Data are representative of two independent experiments. (F) Consensus β-TrCP degron sequence in mouse p19^{Arf} and the corresponding sequences of rat p19^{Arf} and human p14^{Arf}. The conserved region is shaded. Ph, phosphorylation; x, any amino acid. (G) Binding of β-TrCP1 or β-TrCP2 to p19^{Arf} in transfected 293T cells. Cells transiently transfected with expression vectors for FLAG-tagged β-TrCP1 isoform a or β-TrCP2 isoform c or d as well as for hemagglutinin epitope (HA)-tagged p19^{Arf} were lysed and subjected to immunoprecipitation (IP) with antibodies to FLAG. The resulting precipitates as well as the original cell lysates (5% input) were subjected to immunoblot (IB) analysis with antibodies to HA and to FLAG. Band intensities were quantified with ImageJ software. (H) Binding of β-TrCP2 isoform c to p19^{Arf} degron mutants in transfected 293T cells was determined as for panel G. WT, wild type. (I) Left, proliferation of MEFs of the indicated β-TrCP2 genotypes infected with retroviruses encoding three different shRNAs targeting p19^{Arf} mRNA (or with the corresponding empty virus). The cells were infected with the shRNA retroviruses before the Cre recombinase retrovirus. Data are means ± SEM for three independent experiments. Right, RT-qPCR analysis of β-TrCP2 mRNA and immunoblot analysis of p19^{Arf} in the indicated MEFs. RT-qPCR data are means ± SEM for two different experiments. (J) Binding of β-TrCP2 isoform c to mouse p19^{Arf} or human p14^{Arf} in transfected 293T cells was determined as for panel G.

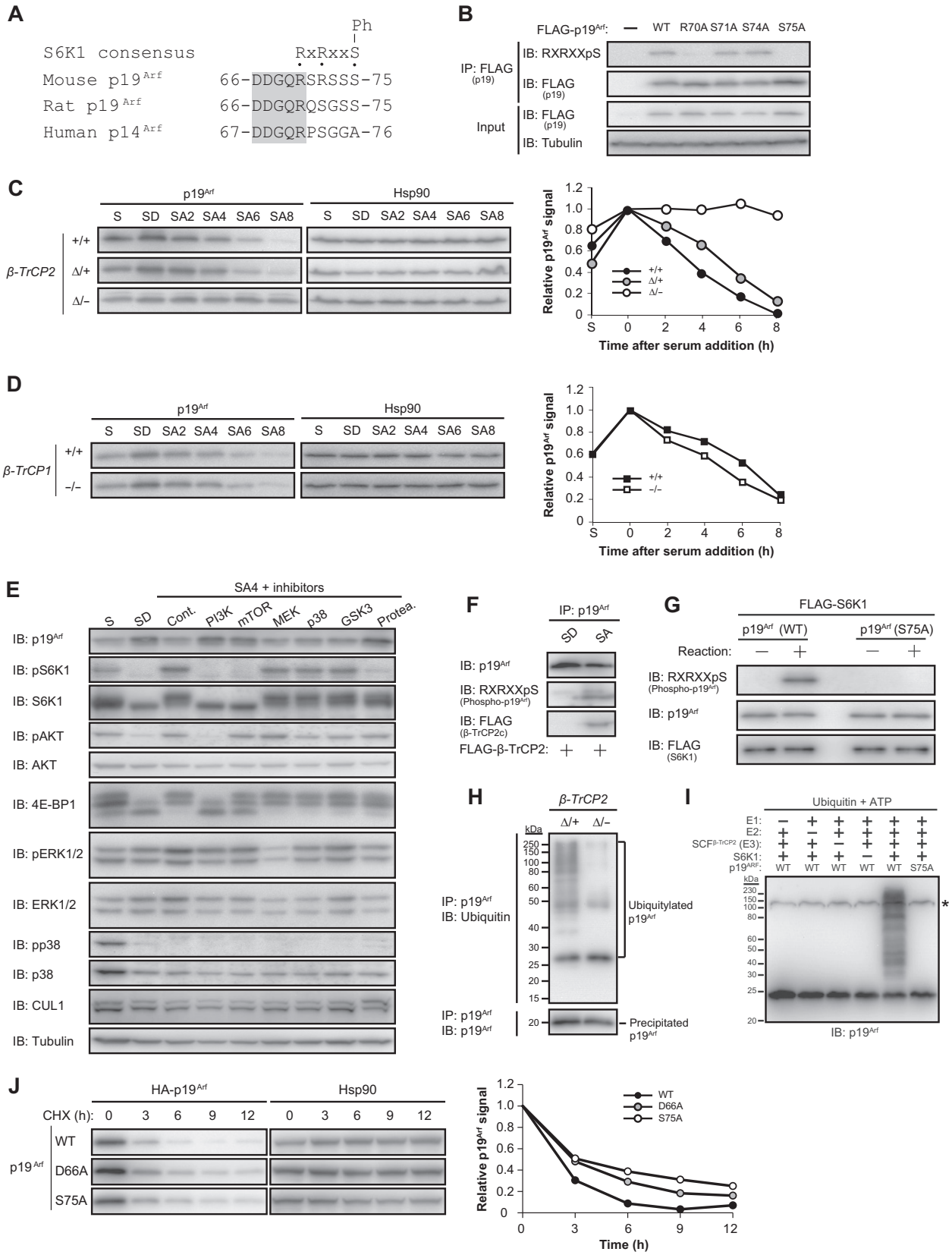

FIG 3 Phosphorylation of p19^{Arf} by S6K1 promotes its binding to β-TrCP2 and degradation. (A) Consensus S6K1 phosphorylation sequence in mouse p19^{Arf} and the corresponding sequences of rat p19^{Arf} and human p14^{Arf}. The conserved region is shaded. Ph, phosphorylation site; x, any amino acid. (B) Analysis of p19^{Arf} phosphorylation in 293T cells. Cells were transiently transfected with an expression vector for FLAG-tagged WT or mutant forms of p19^{Arf}, lysed, and

ious substrates of β-TrCP1 or β-TrCP2. However, no substantial accumulation of such proteins in β-*TrCP2*$^{\Delta/-}$ MEFs was apparent (Fig. 2A). We next examined the expression of negative regulators of the cell cycle and found that p19^{Arf}, p53, p21^{Cip1}, and p27^{Kip1} were upregulated in the β-TrCP2 knockout MEFs (Fig. 2B). Among these proteins, we focused on p19^{Arf} as a potential novel substrate of β-TrCP2 given the following: (i) p19^{Arf} contains a β-TrCP degron sequence (Fig. 2F), a motif to which β-TrCP has been shown to bind; (ii) the abundance of p19^{Arf} mRNA was not markedly increased in β-*TrCP2*$^{\Delta/-}$ MEFs (Fig. 2C), suggesting that p19^{Arf} accumulation did not result from transcriptional regulation; and (iii) induction of p53 and p21^{Cip1} in the mutant MEFs was likely the result of p19^{Arf} accumulation (28), a notion supported by the observation that the amount of p21^{Cip1} mRNA was increased in β-*TrCP2*$^{\Delta/-}$ MEFs (Fig. 2D). Cycloheximide chase analysis revealed that p19^{Arf} was stabilized in these mutant MEFs (Fig. 2E). Furthermore, coimmunoprecipitation analysis revealed that p19^{Arf} bound to β-TrCP2 in transfected 293T cells (Fig. 2G), and this binding was found to require the β-TrCP degron sequence of p19^{Arf} (Fig. 2F and H). Of note, the extent of p19^{Arf} binding to β-TrCP2 was two to three times as great as that to β-TrCP1 (Fig. 2G). These results were thus consistent with the notion that p19^{Arf} is a specific substrate of β-TrCP2. We also found that RNA interference (RNAi)-mediated depletion of p19^{Arf} reversed the proliferation defect of β-TrCP2-deficient cells (Fig. 2I), suggesting that p19^{Arf} is a key substrate of β-TrCP2 in the regulation of cell proliferation. Comparison of the β-TrCP degron sequence of mouse p19^{Arf} with the corresponding sequences of rat and human Arf revealed that the serine residue at the sixth amino acid position of the β-TrCP degron is replaced in the latter two proteins with a different amino acid (glutamine and proline, respectively), suggesting that the rat and human proteins do not contain a functional β-TrCP degron. Consistent with this observation, coimmunoprecipitation analysis revealed that human p14^{Arf} did not bind to β-TrCP2 in transfected 293T cells (Fig. 2J). Together, these data thus indicated that β-TrCP2, but not β-TrCP1, mediates the degradation of p19^{Arf} in MEFs and that the proliferative defect of β-TrCP2 knockout MEFs is dependent on the abnormal accumulation of p19^{Arf}.

Phosphorylation of p19^{Arf} by S6K1 promotes its association with β-TrCP2 and degradation. The β-TrCP degron must be phosphorylated to be recognized by β-TrCP1 or β-TrCP2. Our analysis of the amino acid sequence of mouse p19^{Arf} revealed that a consensus sequence for S6K1 phosphorylation overlaps with the β-TrCP degron (Fig. 3A), suggesting that S6K1 might be responsible for phosphorylation of the latter motif. Immunoblot analysis with antibodies specific for the phosphorylated S6K1 consensus sequence (29) revealed that the β-TrCP degron of p19^{Arf} was indeed phosphorylated in transfected 293T cells and that this phosphorylation required the RXRXXS S6K1 consensus motif (Fig. 3B). S6K1 is phosphorylated and activated by mTOR, whose activity in turn is regulated by nutrient availability (3). Given that nutrient-rich conditions activate the mTOR-S6K1 axis and thereby likely induce p19^{Arf} phosphorylation, we hypothesized that serum stimulation might result in p19^{Arf} ubiquitylation by SCF$^{\beta\text{-TrCP2}}$ and its consequent degradation. Loss of β-TrCP2, but not that of β-TrCP1, abrogated p19^{Arf} degradation induced by serum stimulation in MEFs (Fig. 3C and D), providing further support for a functional difference between β-TrCP paralogs as well as indicating the necessity of β-TrCP2 for p19^{Arf} degradation under nutrient-rich conditions. Furthermore, inhibition of mTOR or its upstream activator PI3K abolished the serum-induced downregulation of p19^{Arf}, whereas other kinase inhibitors had no such effect (Fig. 3E), confirming a role for the mTOR-S6K1 axis in p19^{Arf} degradation. We also found that serum stimulation indeed induced p19^{Arf} phosphorylation as well as the association of phosphorylated p19^{Arf} with FLAG-tagged β-TrCP2 in cells (Fig. 3F) and that S6K1 phosphorylated p19^{Arf} *in vitro* in a manner dependent on the putative S6K1 phosphorylation site (Fig. 3G). In addition, the extent of p19^{Arf} ubiquitylation in MEFs was markedly reduced in the absence of β-TrCP2 (Fig. 3H), and the purified SCF$^{\beta\text{-TrCP2}}$ complex ubiquitylated p19^{Arf} *in vitro* in an E1-, E2-, and S6K1-dependent manner (Fig. 3I). Furthermore, p19^{Arf} mutants that are not able to interact with β-TrCP2 or to be phosphorylated by S6K1 were more stable than the WT protein in mouse NIH 3T3 cells (Fig. 3J). Together, these observations indicated that phosphorylation of p19^{Arf} by S6K1 under nutrient-rich conditions results in its β-TrCP2-mediated ubiquitylation and degra-

subjected to immunoprecipitation with antibodies to FLAG followed by immunoblot analysis with antibodies to the phosphorylated S6K1 consensus phosphorylation sequence (RXRXXpS) and to FLAG. (C and D) Left, immunoblot analysis of p19^{Arf} in MEFs of the indicated β-TrCP2 (C) or β-TrCP1 (D) genotypes after serum deprivation for 2 days and subsequent serum stimulation for the indicated times. Right, Relative p19^{Arf} abundance normalized by Hsp90 abundance as determined by quantitation of immunoblot signals. Data are representative of two independent experiments. S, normal serum condition (10% serum) without prior serum deprivation; SD, serum-depleted condition (0.1% serum for 2 days); SA, serum-activated condition (10% serum) for the indicated number of hours after serum deprivation. (E) Immunoblot analysis of signaling molecules in WT MEFs. Cells were deprived of serum as for panel C, incubated with kinase inhibitors for the last 30 min of serum deprivation, and then stimulated with serum for 4 h in the continued presence of kinase inhibitors before immunoblot analysis with antibodies to total or phosphorylated (p) forms of the indicated proteins. Kinase inhibitors: 50 μM LY294002 (PI3K), 100 nM rapamycin (mTOR), 20 μM U0126 (MEK), 20 μM SB203580 (p38 mitogen-activated protein kinase [MAPK]), and 5 μM GSK inhibitor (GSK3). The proteasome inhibitor MG132 (Protea.) (10 μM) was also examined, and 0.1% dimethyl sulfoxide was used as a control (Cont.). (F) Binding of endogenous phosphorylated p19^{Arf} to FLAG–β-TrCP2 in MEFs. MEFs infected with a retrovirus encoding FLAG-tagged β-TrCP2 isoform c were deprived of serum and then stimulated with serum for 1 h as for panel C. Cell lysates were subjected to immunoprecipitation with antibodies to p19^{Arf} followed by immunoblot analysis with the indicated antibodies. (G) *In vitro* phosphorylation of p19^{Arf} by S6K1. Recombinant WT or S75A mutant forms of p19^{Arf} and a FLAG-tagged constitutively active form of S6K1 were incubated for 0 or 5 min in a kinase reaction buffer and then subjected to immunoblot analysis with the indicated antibodies. (H) Ubiquitylation of p19^{Arf} in MEFs. MEFs of the indicated genotypes were deprived of serum for 2 days, exposed to 10 μM MG132 (to prevent degradation of p19^{Arf}) for the last 3 h of serum deprivation, and then stimulated with serum in the continued presence of MG132 for 1 h. Cell lysates were subjected to immunoprecipitation with antibodies to p19^{Arf} under denaturing conditions followed by immunoblot analysis with antibodies to ubiquitin or to p19^{Arf}. (I) Ubiquitylation of p19^{Arf} by SCF$^{\beta\text{-TrCP2}}$ *in vitro*. The indicated reaction mixture components were incubated for 120 min at 37°C and then subjected to immunoblot analysis with antibodies to p19^{Arf}. *, nonspecific band. (J) Left, NIH 3T3 cells infected with retroviruses encoding HA-tagged WT p19^{Arf} or mutant forms that cannot interact with β-TrCP2 (D66A) or cannot be phosphorylated by S6K1 (S75A) were incubated with cycloheximide (CHX) (25 μg/ml) for the indicated times and then subjected to immunoblot analysis with antibodies to HA and to Hsp90. Right, relative HA-p19^{Arf} abundance normalized by Hsp90 abundance as determined by quantitation of immunoblot signals with ImageJ software.

dation and consequent promotion of cell proliferation. Importantly, β-TrCP1 does not share this function of β-TrCP2.

Disruption of the β-TrCP2 gene induces embryonic lethality accompanied by p19^{Arf} accumulation in the yolk sac. Our finding that p19^{Arf} accumulation is a major contributor to the arrest of cell proliferation in β-TrCP2-deficient MEFs led us to examine whether p19^{Arf} is also a key substrate of β-TrCP2 in animals, especially with regard to the embryonic mortality of β-TrCP2 knockout mice. Disruption of the mouse β-TrCP2 gene by deletion of exons 5 and 6 was not compatible with embryonic development (Fig. 4A, B, and E), whereas both male and female β-*TrCP2*$^{+/-}$ mice showed no obvious abnormalities, with fertility and growth rates similar to those of WT controls (data not shown).

To determine the developmental stage at which β-TrCP2 deficiency results in embryonic lethality, we analyzed embryos of heterozygote intercrosses at various stages of gestation. The β-*TrCP2*$^{+/+}$/β-*TrCP2*$^{+/-}$/β-*TrCP2*$^{-/-}$ embryo genotype ratio was 1:2:1 up to E9.5, but no viable β-*TrCP2*$^{-/-}$ embryos were detected beyond E10.5 (Fig. 4E). Deletion of the β-TrCP2 gene and loss of β-TrCP2 mRNA in homozygous mutant embryos were confirmed by genomic PCR and RT-qPCR analyses, respectively (Fig. 4C and D). β-*TrCP2*$^{-/-}$ embryos at E9.5 showed a developmental delay, and they were resorbed at E10.5 (Fig. 4F). These data thus showed that homozygosity for the β-TrCP2 null mutation results in developmental arrest and embryonic death before E10.5 and that β-TrCP1 is not able to compensate for the loss of β-TrCP2.

To investigate whether the β-TrCP2 regulation of p19^{Arf} observed in MEFs also operates in a more physiological setting, we examined β-TrCP2 knockout embryos further. Whereas p19^{Arf} is expressed specifically in the yolk sac (30), not in the embryo proper, we found that β-TrCP1 and β-TrCP2 mRNAs were present in both compartments of WT embryos (Fig. 4G). The abundance of p19^{Arf} in the yolk sac was greatly increased by β-TrCP2 knockout (Fig. 4H), indicating that p19^{Arf} is a physiological substrate of β-TrCP2.

Finally, we tested the possibility that p19^{Arf} accumulation is the primary cause of embryonic death in β-TrCP2 knockout mice by crossing β-*TrCP2*$^{+/-}$ mice with *Cdkn2a*$^{-/-}$ mice, which lack both p19^{Arf} and p16^{Ink4a} (19, 20). However, β-*TrCP2*$^{-/-}$; *Cdkn2a*$^{-/-}$ embryos manifested the same phenotype as β-*TrCP2*$^{-/-}$ embryos (Fig. 4I), indicating that p19^{Arf} accumulation *per se* is not sufficient to account for the embryonic lethality of β-TrCP2 ablation and that additional substrates of β-TrCP2 that contribute to such lethality remain to be identified.

DISCUSSION

β-TrCP is one of the most-studied F-box proteins, as exemplified by the identification of >50 substrates to date in mammals. However, the physiologically important substrates of β-TrCP have remained unclear, in part because of the lack of an animal model completely deficient in β-TrCP1 and β-TrCP2 (31).

We previously generated β-TrCP1 knockout mice and found that they manifested only minor defects (16). We have now generated β-TrCP2 knockout mice and found that the most obvious phenotype is embryonic mortality, despite the fact that the β-TrCP1 gene is intact in these animals. This unexpected finding led us to reevaluate the prevailing view that β-TrCP1 and β-TrCP2 are functionally redundant and essentially indistinguishable. Our subsequent demonstration that β-TrCP2, but not β-TrCP1, positively regulates cell proliferation by targeting p19^{Arf} for ubiquitylation and degradation under nutrient-rich conditions revealed a key functional difference between these two proteins. Furthermore, loss of p19^{Arf} did not rescue the embryonic lethality of β-TrCP2 ablation, suggesting that additional substrates targeted by β-TrCP2 but not by β-TrCP1 contribute to this phenotype in mouse embryos.

Our finding that the arrest of cell proliferation induced by loss of β-TrCP2 in MEFs was completely reversed by concomitant depletion of p19^{Arf} indicates that the regulation of p19^{Arf} by β-TrCP2 is likely to play a key role in tissues other than the yolk sac, in particular in adult tissues under conditions in which activation of the mTOR-S6K1 axis controls cell proliferation. Further studies with our conditional knockout system should shed light on the function of β-TrCP2 in adult mice.

At least two other ubiquitin ligases target p19^{Arf} for degradation: TRIP12 (ULF) and SIVA1 bind to and mediate the ubiquitylation and degradation of p19^{Arf} (32–34). Why do mouse cells express three different ubiquitin ligases for p19^{Arf}? TRIP12 and SIVA1 do not appear to require any modification of p19^{Arf} in order to mediate its ubiquitylation. Genotoxic stress induces the degradation of p19^{Arf} by TRIP12, whereas SIVA1 is induced by p53 and its downregulation of p19^{Arf} results in the destabilization of p53, completing a negative feedback loop that limits the level of p53 activation. These observations indicate that TRIP12 and SIVA1 induce the degradation of p19^{Arf} in order to prevent hyperactivation of p53 in response to stress, whereas SCF$^{β\text{-}TrCP2}$-induced p19^{Arf} degradation promotes cell proliferation specifically in response to nutrient availability. Of note, we found that the β-TrCP degron as well as the S6K1 consensus sequence present in mouse p19^{Arf} are disrupted in human p14^{Arf} and rat p19^{Arf} (Fig. 2F and I and 3A), suggesting that the human and rat proteins are not targeted for degradation by β-TrCP2. The reason for this species difference is not clear, but it will be of interest to compare the stabilities of human p14^{Arf} and rat p19^{Arf} with that of mouse p19^{Arf} in cells subject to nutrient stimulation.

We found that S6K1 phosphorylates p19^{Arf} and thereby primes it for degradation. In mammals, S6K1 (RPS6KB1) and its paralog S6K2 (RPS6KB2) have been thought to have essentially overlapping functions, with a few exceptions (35). Given that S6K2 is also activated by mTORC1, we cannot exclude the possibility that S6K2 also phosphorylates p19^{Arf}. Importantly, S6K activity is present not only in the cytosol but also in the nucleolus, where most p19^{Arf} resides (36, 37), indicating that S6K might phosphorylate p19^{Arf} in this subnuclear compartment.

Activation of S6K1 and S6K2 requires their mTORC1-mediated phosphorylation, and mTORC1 is activated by the growth factor-induced PI3K-AKT-TSC-Rheb pathway. We thus found that inhibitors of PI3K or mTORC1 suppressed serum-induced p19^{Arf} degradation. This regulation of p19^{Arf} is similar to that of the translation inhibitor PDCD4, which is phosphorylated by S6K and subsequently ubiquitylated by β-TrCP to facilitate translation (38). Furthermore, Deptor, a shared component of mTORC1 and mTORC2 and negative regulator of mTOR, is also ubiquitylated by β-TrCP after its phosphorylation by the combination either of S6K1 and RSK1 (RPS6KA1) or of mTOR and casein kinase 1α (CK1α) (39–41). In addition, the protein phosphatase PHLPP1, which inactivates AKT, was found to serve as a substrate of β-TrCP after its phosphorylation by CK1 and GSK-3β (42). These

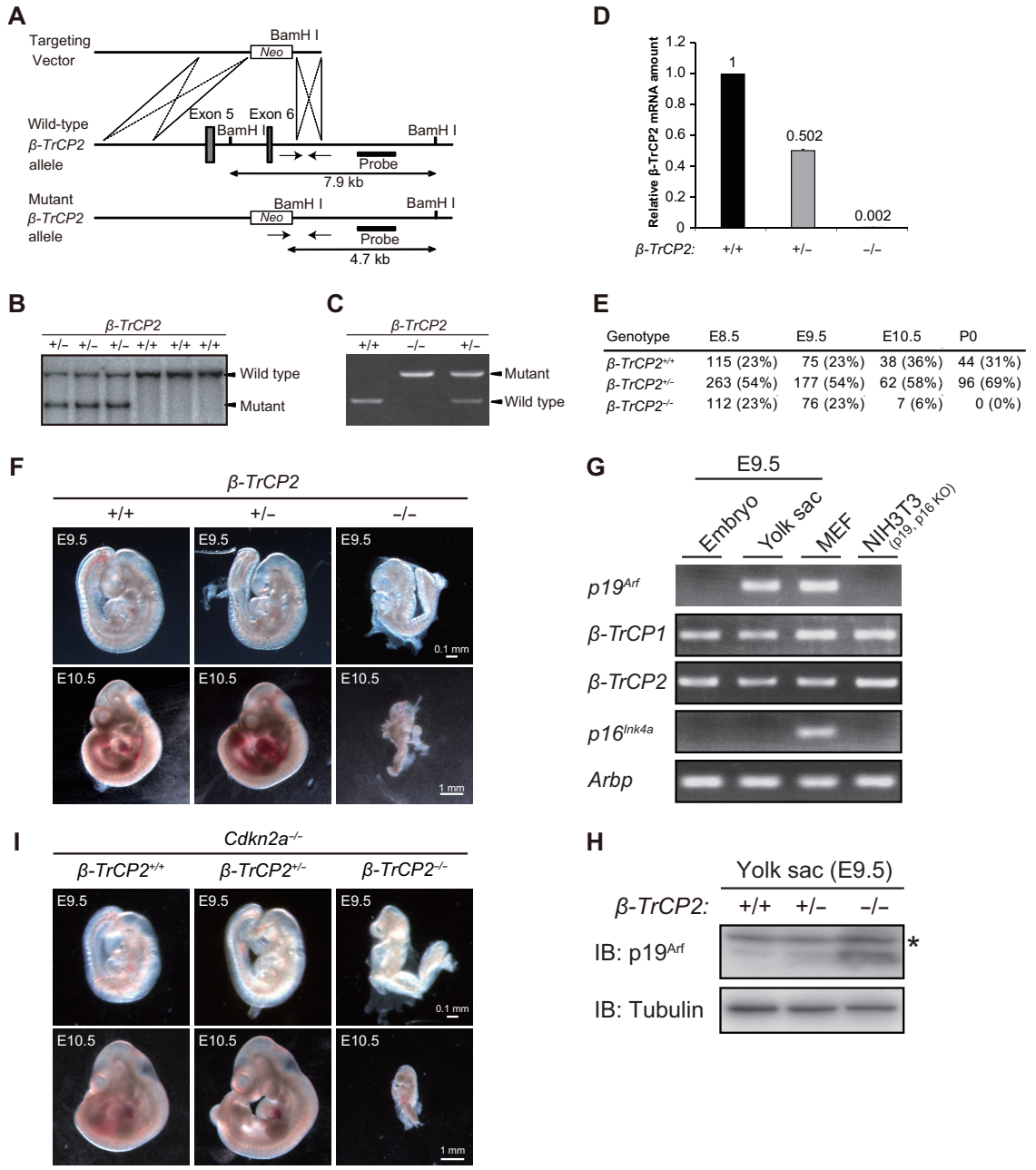

FIG 4 Disruption of the β-TrCP2 gene induces embryonic mortality in mice accompanied by p19^{Arf} accumulation in the yolk sac. (A) Structures of the targeting vector, the mouse β-TrCP2 gene locus, and the mutant allele resulting from homologous recombination. Exons 5 and 6 of the β-TrCP2 gene are shown as filled boxes. A genomic fragment used as a probe for Southern blot analysis is also shown, together with the expected sizes of hybridizing BamHI fragments of the WT and mutant alleles. Genotyping primers are indicated by arrows. *neo*, neomycin transferase gene linked to the phosphoglycerate kinase gene promoter. (B) Southern blot analysis of BamHI-digested tail DNA from adult mice of the indicated genotypes. (C) Genomic PCR analysis of E9.5 embryos of the indicated genotypes. (D) RT-qPCR analysis of β-TrCP2 mRNA in E9.5 embryos of the indicated genotypes. Data are means ± SEM for two embryos of each genotype. (E) Genotyping of embryos (E8.5, E9.5, and E10.5) and neonates (P0) obtained from intercrosses of β-*TrCP2*$^{+/-}$ mice. (F) Gross appearance of E9.5 and E10.5 embryos of the indicated genotypes. Scale bars, 0.1 mm (E9.5) or 1 mm (E10.5). (G) RT-PCR analysis of p19^{Arf}, β-TrCP1, β-TrCP2, and p16^{Ink4a} mRNAs in the WT yolk sac and embryo proper at E9.5. *Arbp* served as an internal control, and WT MEFs and NIH 3T3 cells (in which the *Cdkn2a* locus is deleted) served as a control for gene expression. (H) Immunoblot analysis of p19^{Arf} in the E9.5 yolk sacs of the indicated genotypes. *, nonspecific band. (I) Gross appearance of E9.5 and E10.5 embryos of the indicated genotypes. Scale bars, 0.1 mm (E9.5) or 1 mm (E10.5).

observations indicate that β-TrCP plays a key role in mTOR signaling by facilitating translation (via PDCD4 degradation) and proliferation (via p19^{Arf} degradation) as well as by amplifying mTOR activity (via Deptor degradation) and upstream AKT activity (via PHLPP1 degradation), although the reason why β-TrCP1 does not participate in p19^{Arf} degradation is unclear.

Sustained activation of mTORC1 induced by ablation of TSC1 and TSC2 was shown to reduce the half-life of p19^{Arf}

(consistent with our present findings) but also to facilitate translation of $p19^{Arf}$ mRNA, the net result of which was the upregulation of $p19^{Arf}$ (43). These effects might constitute a mechanism of cellular adaptation that prevents overproliferation in response to hypernutrition. Another example of $p19^{Arf}$-dependent cellular adaptation is provided by the observation that moderate expression of c-Myc promotes cell proliferation, whereas its overexpression inhibits proliferation through competitive binding of c-Myc to TRIP12 and consequent accumulation of $p19^{Arf}$ (33).

Together, our findings have revealed that β-TrCP2 has a distinct function not shared by β-TrCP1 both *in vivo* and *in vitro*. Indeed, we did not detect the accumulation of any well-known substrates of β-TrCP in β-*TrCP2*$^{\Delta/-}$ MEFs (Fig. 2A), and cycloheximide chase analysis revealed that none of those examined was stabilized in the mutant cells (data not shown), suggesting that β-TrCP2 is not required for the degradation of these substrates in MEFs in the presence of β-TrCP1. Resolution of the crystal structure of β-TrCP2 should shed light on the molecular underpinnings of this functional disparity between β-TrCP1 and β-TrCP2 and explain why most vertebrates appear to retain two β-TrCP paralogs (44). In addition, we have identified a new mechanism for the regulation of cell proliferation mediated by the mTOR-S6K1 axis. S6K1 thus induces β-TrCP2-dependent degradation of $p19^{Arf}$ and thereby promotes cell proliferation in a nutrient-rich environment. As far as we are aware, this is the first example of the direct regulation of cell proliferation by the mTOR pathway independent of transcription and translation.

ACKNOWLEDGMENTS

We thank T. Kitamura for pMX-puro and Plat-E cells, K. Yumimoto and K. I. Nakayama for sharing unpublished data, Y. Nagasawa and T. Senga for technical assistance, and other laboratory members for discussion.

This work was supported by grants 25891003 and 15K18365 from the Japan Society for the Promotion of Science.

REFERENCES

1. **Laplante M, Sabatini DM.** 2012. mTOR signaling in growth control and disease. Cell **149:**274–293. http://dx.doi.org/10.1016/j.cell.2012.03.017.
2. **Shimobayashi M, Hall MN.** 2014. Making new contacts: the mTOR network in metabolism and signalling crosstalk. Nat Rev Mol Cell Biol **15:**155–162. http://dx.doi.org/10.1038/nrm3757.
3. **Magnuson B, Ekim B, Fingar DC.** 2012. Regulation and function of ribosomal protein S6 kinase (S6K) within mTOR signalling networks. Biochem J **441:**1–21. http://dx.doi.org/10.1042/BJ20110892.
4. **Silvera D, Formenti SC, Schneider RJ.** 2010. Translational control in cancer. Nat Rev Cancer **10:**254–266. http://dx.doi.org/10.1038/nrc2824.
5. **Ma XM, Blenis J.** 2009. Molecular mechanisms of mTOR-mediated translational control. Nat Rev Mol Cell Biol **10:**307–318. http://dx.doi.org/10.1038/nrm2672.
6. **Jewell JL, Guan KL.** 2013. Nutrient signaling to mTOR and cell growth. Trends Biochem Sci **38:**233–242. http://dx.doi.org/10.1016/j.tibs.2013.01.004.
7. **Dowling RJ, Topisirovic I, Alain T, Bidinosti M, Fonseca BD, Petroulakis E, Wang X, Larsson O, Selvaraj A, Liu Y, Kozma SC, Thomas G, Sonenberg N.** 2010. mTORC1-mediated cell proliferation, but not cell growth, controlled by the 4E-BPs. Science **328:**1172–1176. http://dx.doi.org/10.1126/science.1187532.
8. **Mori S, Nada S, Kimura H, Tajima S, Takahashi Y, Kitamura A, Oneyama C, Okada M.** 2014. The mTOR pathway controls cell proliferation by regulating the FoxO3a transcription factor via SGK1 kinase. PLoS One **9:**e88891. http://dx.doi.org/10.1371/journal.pone.0088891.
9. **Nakayama KI, Nakayama K.** 2006. Ubiquitin ligases: cell-cycle control and cancer. Nat Rev Cancer **6:**369–381. http://dx.doi.org/10.1038/nrc1881.
10. **Glickman MH, Ciechanover A.** 2002. The ubiquitin-proteasome proteolytic pathway: destruction for the sake of construction. Physiol Rev **82:**373–428. http://dx.doi.org/10.1152/physrev.00027.2001.
11. **Cardozo T, Pagano M.** 2004. The SCF ubiquitin ligase: insights into a molecular machine. Nat Rev Mol Cell Biol **5:**739–751. http://dx.doi.org/10.1038/nrm1471.
12. **Fuchs SY, Spiegelman VS, Kumar KG.** 2004. The many faces of β-TrCP E3 ubiquitin ligases: reflections in the magic mirror of cancer. Oncogene **23:**2028–2036. http://dx.doi.org/10.1038/sj.onc.1207389.
13. **Frescas D, Pagano M.** 2008. Deregulated proteolysis by the F-box proteins SKP2 and β-TrCP: tipping the scales of cancer. Nat Rev Cancer **8:**438–449. http://dx.doi.org/10.1038/nrc2396.
14. **Skaar JR, D'Angiolella V, Pagan JK, Pagano M.** 2009. SnapShot: F box proteins II. Cell **137:**1358. http://dx.doi.org/10.1016/j.cell.2009.05.040.
15. **Guardavaccaro D, Kudo Y, Boulaire J, Barchi M, Busino L, Donzelli M, Margottin-Goguet F, Jackson PK, Yamasaki L, Pagano M.** 2003. Control of meiotic and mitotic progression by the F box protein β-Trcp1 in vivo. Dev Cell **4:**799–812. http://dx.doi.org/10.1016/S1534-5807(03)00154-0.
16. **Nakayama K, Hatakeyama S, Maruyama S, Kikuchi A, Onoe K, Good RA, Nakayama KI.** 2003. Impaired degradation of inhibitory subunit of NF-κB (IκB) and β-catenin as a result of targeted disruption of the β-TrCP1 gene. Proc Natl Acad Sci U S A **100:**8752–8757. http://dx.doi.org/10.1073/pnas.1133216100.
17. **Maruyama S, Hatakeyama S, Nakayama K, Ishida N, Kawakami K, Nakayama K.** 2001. Characterization of a mouse gene (*Fbxw6*) that encodes a homologue of *Caenorhabditis elegans* SEL-10. Genomics **78:**214–222. http://dx.doi.org/10.1006/geno.2001.6658.
18. **Nakayama K, Ishida N, Shirane M, Inomata A, Inoue T, Shishido N, Horii I, Loh DY, Nakayama K.** 1996. Mice lacking p27(Kip1) display increased body size, multiple organ hyperplasia, retinal dysplasia, and pituitary tumors. Cell **85:**707–720. http://dx.doi.org/10.1016/S0092-8674(00)81237-4.
19. **Serrano M, Lee H, Chin L, Cordon-Cardo C, Beach D, DePinho RA.** 1996. Role of the INK4a locus in tumor suppression and cell mortality. Cell **85:**27–37. http://dx.doi.org/10.1016/S0092-8674(00)81079-X.
20. **Tamase A, Muraguchi T, Naka K, Tanaka S, Kinoshita M, Hoshii T, Ohmura M, Shugo H, Ooshio T, Nakada M, Sawamoto K, Onodera M, Matsumoto K, Oshima M, Asano M, Saya H, Okano H, Suda T, Hamada J, Hirao A.** 2009. Identification of tumor-initiating cells in a highly aggressive brain tumor using promoter activity of nucleostemin. Proc Natl Acad Sci U S A **106:**17163–17168. http://dx.doi.org/10.1073/pnas.0905016106.
21. **Hosogane M, Funayama R, Nishida Y, Nagashima T, Nakayama K.** 2013. Ras-induced changes in H3K27me3 occur after those in transcriptional activity. PLoS Genet **9:**e1003698. http://dx.doi.org/10.1371/journal.pgen.1003698.
22. **Morita S, Kojima T, Kitamura T.** 2000. Plat-E: an efficient and stable system for transient packaging of retroviruses. Gene Ther **7:**1063–1066. http://dx.doi.org/10.1038/sj.gt.3301206.
23. **Nakagawa T, Lv L, Nakagawa M, Yu Y, Yu C, D'Alessio AC, Nakayama K, Fan HY, Chen X, Xiong Y.** 2015. CRL4(VprBP) E3 ligase promotes monoubiquitylation and chromatin binding of TET dioxygenases. Mol Cell **57:**247–260. http://dx.doi.org/10.1016/j.molcel.2014.12.002.
24. **Nakagawa T, Xiong Y.** 2011. X-linked mental retardation gene *CUL4B* targets ubiquitylation of H3K4 methyltransferase component WDR5 and regulates neuronal gene expression. Mol Cell **43:**381–391. http://dx.doi.org/10.1016/j.molcel.2011.05.033.
25. **Kaneko-Oshikawa C, Nakagawa T, Yamada M, Yoshikawa H, Matsumoto M, Yada M, Hatakeyama S, Nakayama K, Nakayama KI.** 2005. Mammalian E4 is required for cardiac development and maintenance of the nervous system. Mol Cell Biol **25:**10953–10964. http://dx.doi.org/10.1128/MCB.25.24.10953-10964.2005.
26. **Schalm SS, Blenis J.** 2002. Identification of a conserved motif required for mTOR signaling. Curr Biol **12:**632–639. http://dx.doi.org/10.1016/S0960-9822(02)00762-5.
27. **Zhang J, Gao Z, Yin J, Quon MJ, Ye J.** 2008. S6K directly phosphorylates IRS-1 on Ser-270 to promote insulin resistance in response to TNF-α signaling through IKK2. J Biol Chem **283:**35375–35382. http://dx.doi.org/10.1074/jbc.M806480200.
28. **Lowe SW, Sherr CJ.** 2003. Tumor suppression by Ink4a-Arf: progress and puzzles. Curr Opin Genet Dev **13:**77–83. http://dx.doi.org/10.1016/S0959-437X(02)00013-8.
29. **Moritz A, Li Y, Guo A, Villen J, Wang Y, MacNeill J, Kornhauser J, Sprott K, Zhou J, Possemato A, Ren JM, Hornbeck P, Cantley LC, Gygi**

SP, Rush J, Comb MJ. 2010. Akt-RSK-S6 kinase signaling networks activated by oncogenic receptor tyrosine kinases. Sci Signal **3:**ra64.

30. **Jerome-Majewska LA, Jenkins GP, Ernstoff E, Zindy F, Sherr CJ, Papaioannou VE.** 2005. Tbx3, the ulnar-mammary syndrome gene, and Tbx2 interact in mammary gland development through a p19Arf/p53-independent pathway. Dev Dyn **234:**922–933. http://dx.doi.org/10.1002/dvdy.20575.
31. **Zhou W, Wei W, Sun Y.** 2013. Genetically engineered mouse models for functional studies of SKP1-CUL1-F-box-protein (SCF) E3 ubiquitin ligases. Cell Res **23:**599–619. http://dx.doi.org/10.1038/cr.2013.44.
32. **Chen D, Shan J, Zhu WG, Qin J, Gu W.** 2010. Transcription-independent ARF regulation in oncogenic stress-mediated p53 responses. Nature **464:**624–627. http://dx.doi.org/10.1038/nature08820.
33. **Chen D, Kon N, Zhong J, Zhang P, Yu L, Gu W.** 2013. Differential effects on ARF stability by normal versus oncogenic levels of c-Myc expression. Mol Cell **51:**46–56. http://dx.doi.org/10.1016/j.molcel.2013.05.006.
34. **Wang X, Zha M, Zhao X, Jiang P, Du W, Tam AY, Mei Y, Wu M.** 2013. Siva1 inhibits p53 function by acting as an ARF E3 ubiquitin ligase. Nat Commun **4:**1551. http://dx.doi.org/10.1038/ncomms2533.
35. **Pardo OE, Seckl MJ.** 2013. S6K2: the neglected S6 kinase family member. Front Oncol **3:**191. http://dx.doi.org/10.3389/fonc.2013.00191.23898460.
36. **Zhang Y, Xiong Y.** 1999. Mutations in human ARF exon 2 disrupt its nucleolar localization and impair its ability to block nuclear export of MDM2 and p53. Mol Cell **3:**579–591. http://dx.doi.org/10.1016/S1097-2765(00)80351-2.
37. **Pende M, Um SH, Mieulet V, Sticker M, Goss VL, Mestan J, Mueller M, Fumagalli S, Kozma SC, Thomas G.** 2004. S6K1$^{-/-}$/S6K2$^{-/-}$ mice exhibit perinatal lethality and rapamycin-sensitive 5′-terminal oligopyrimidine mRNA translation and reveal a mitogen-activated protein kinase-dependent S6 kinase pathway. Mol Cell Biol **24:**3112–3124. http://dx.doi.org/10.1128/MCB.24.8.3112-3124.2004.
38. **Dorrello NV, Peschiaroli A, Guardavaccaro D, Colburn NH, Sherman NE, Pagano M.** 2006. S6K1- and βTRCP-mediated degradation of PDCD4 promotes protein translation and cell growth. Science **314:**467–471. http://dx.doi.org/10.1126/science.1130276.
39. **Duan S, Skaar JR, Kuchay S, Toschi A, Kanarek N, Ben-Neriah Y, Pagano M.** 2011. mTOR generates an auto-amplification loop by triggering the βTrCP- and CK1α-dependent degradation of DEPTOR. Mol Cell **44:**317–324. http://dx.doi.org/10.1016/j.molcel.2011.09.005.
40. **Gao D, Inuzuka H, Tan MK, Fukushima H, Locasale JW, Liu P, Wan L, Zhai B, Chin YR, Shaik S, Lyssiotis CA, Gygi SP, Toker A, Cantley LC, Asara JM, Harper JW, Wei W.** 2011. mTOR drives its own activation via SCF$^{\beta TrCP}$-dependent degradation of the mTOR inhibitor DEPTOR. Mol Cell **44:**290–303. http://dx.doi.org/10.1016/j.molcel.2011.08.030.
41. **Zhao Y, Xiong X, Sun Y.** 2011. DEPTOR, an mTOR inhibitor, is a physiological substrate of SCF$^{\beta TrCP}$ E3 ubiquitin ligase and regulates survival and autophagy. Mol Cell **44:**304–316. http://dx.doi.org/10.1016/j.molcel.2011.08.029.
42. **Li X, Liu J, Gao T.** 2009. β-TrCP-mediated ubiquitination and degradation of PHLPP1 are negatively regulated by Akt. Mol Cell Biol **29:**6192–6205. http://dx.doi.org/10.1128/MCB.00681-09.
43. **Miceli AP, Saporita AJ, Weber JD.** 2012. Hypergrowth mTORC1 signals translationally activate the ARF tumor suppressor checkpoint. Mol Cell Biol **32:**348–364. http://dx.doi.org/10.1128/MCB.06030-11.
44. **Wotton KR, Weierud FK, Dietrich S, Lewis KE.** 2008. Comparative genomics of Lbx loci reveals conservation of identical Lbx ohnologs in bony vertebrates. BMC Evol Biol **8:**171.45. http://dx.doi.org/10.1186/1471-2148-8-171.